Electronic Supplementary Material (ESI) for Catalysis Science & Technology.

Electronic Supplementary Information (ESI†)

Fabrication of Ag/Mn_3O_4 nano-architectures for the one-step selective oxidation of 3-picoline to niacin: a key to vitamin B_3 production

Shilpi Ghosh, Shankha Shubhra Acharyya, Sachin Kumar Sharma and Rajaram Bal*

*Catalytic Conversion & Processes Division, CSIR-Indian Institute of Petroleum, Dehradun-248005, India. E-mail: raja@iip.res.in; Fax: +91 135 2660202; Tel: +91 135 2525917

CHARACTERIZATION TECHNIQUES

Powder X-ray diffraction patterns were collected on a Bruker D8 advance X-ray diffractometer fitted with a Lynx eye high-speed strip detector and a Cu K radiation source using Cu Ka radiation with a wavelength of 1.5418 Å. Diffraction patterns in the 2-80° regions were recorded at a rate of 0.5 degrees (2θ) per minute. The resulting XRD profiles were analyzed to identify the crystal phase of the compound using reference standards. The line width of the most intense XRD peak was taken for estimation of crystallite size by the Scherrer equation. Scanning electron microscopy images were taken on a FEI Quanta 200 F, using tungsten filament doped with lanthanumhexaboride (LaB_6) as an x-ray source, fitted with an ETD detector with high vacuum mode using secondary electrons and an acceleration tension of 10 or 30 kV. Samples were analyzed by spreading them on a carbon tape. Energy dispersive X-ray spectroscopy (EDX) was used in connection with SEM for the elemental analysis. The elemental mapping was also collected with the same spectrophotometer. Samples were subjected to scanning electron microscope analysis to understand the shape, size, and morphology properties. The particle size and distribution of the samples were analyzed by TEM, JEOL JEM 2100 microscope, and samples were prepared by mounting an ethanol-dispersed sample on a lacey carbon Formvar coated Cu grid. X-Ray photoelectron spectra were recorded on a Thermo Scientific K-Alpha X-Ray photoelectron spectrometer and binding energies (±0.1 eV) were determined. The resulting spectra were analyzed to identify the different oxidation states of the silver and manganese ions present in the sample. Prior to the analysis, the spectra were calibrated with reference to C1s observed at a binding energy of 284.5 eV. Chemical analyses of the metallic constituents were carried out by Inductively Coupled Plasma Atomic Emission Spectrometer; model: PS 3000 uv, (DRE), Leeman Labs, Inc, (USA). Raman Spectra was measured at 298K by using a Laser Raman Spectrometer (JASCO, NRS-3100) with the 532 nm lines from a diode-pumped solid-state laser for excitation. The FTIR spectra were recorded on a Thermo Nicolet 8700 (USA) instrument with the operating conditions: resolution: 4 cm^{-1}, scan: 36, operating temperature: 23-25 °C and the frequency range: 4000-400cm^{-1}.UV-vis spectra were recorded in air at room temperature using Shimadzu UV-Visible Spectrophotometer (Serial No. A11665101641; Model: UV-2600 230 V, with a diffuse reflectance accessory, in the 200-800 nm wavelength range. UV Probe 2.43 software was used for analysis. Anhydrous $BaSO_4$ was used as a reference. The Kubelka Munk function F(R) was plotted against the wavelength (in nm).

Table S1.

Mn-Species	Corresponding BE (eV)	Corresponding area (after deconvolution)
Mn^{3+} $2p_{3/2}$	641.63	3937.18
Mn^{2+} $2p_{3/2}$	643.09	2093
Mn^{3+} $2p_{1/2}$	652.9	2930.83
Mn^{2+} $2p_{1/2}$	654.83	1800.2

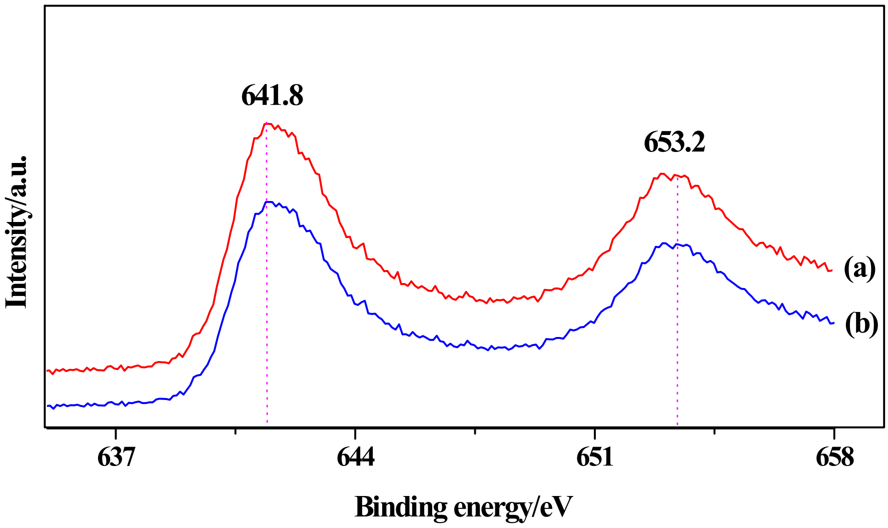

Figure S1. Mn 2p core-level spectra (XPS) of (a) fresh and (b) spent Ag-Mn nano-rod catalyst.

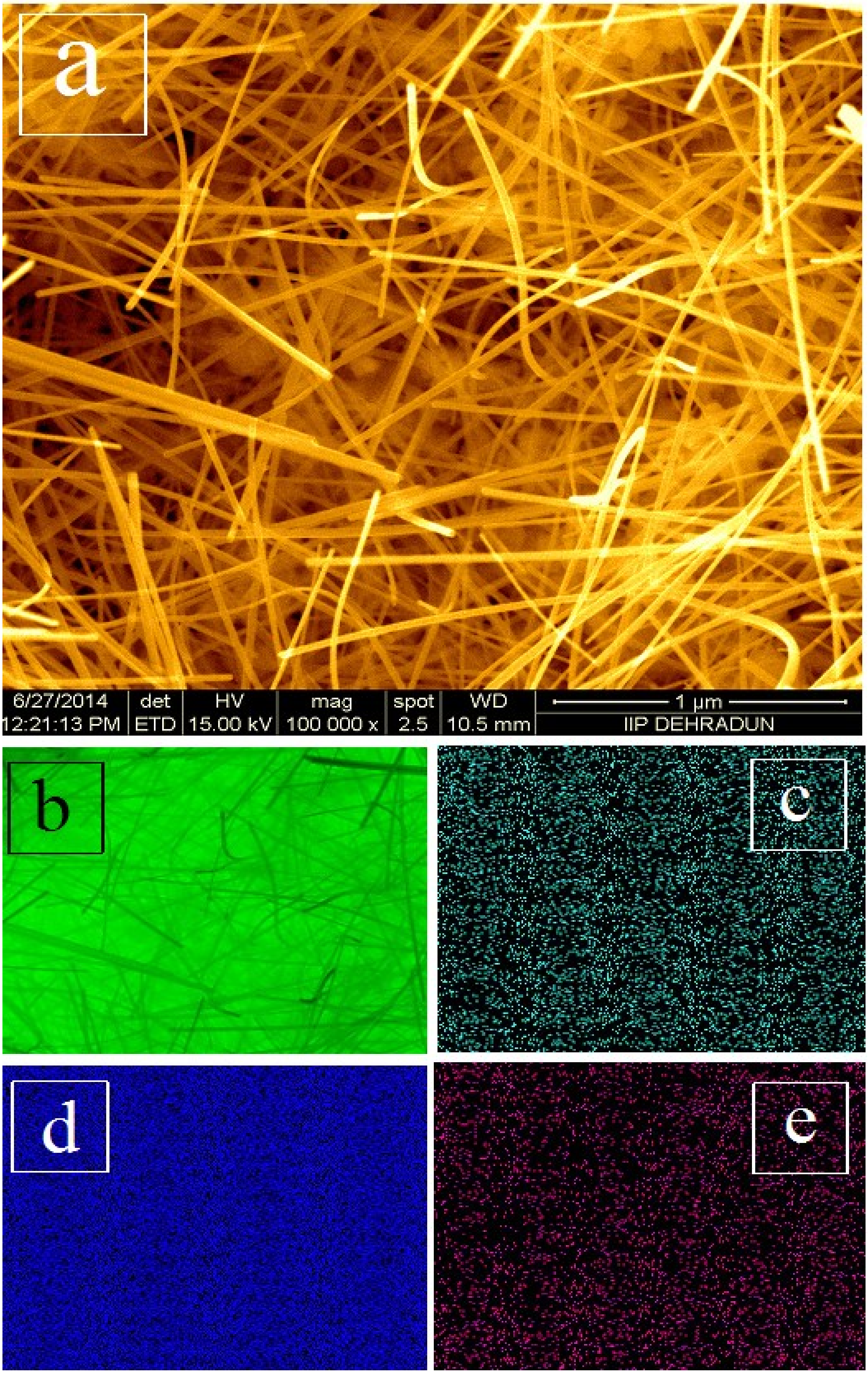

Figure S2. (a) SEM image (repeat of Fig. 4a, Main), (b) SEM-elemental mapping and SEM-elemental mapping of (c) Ag, (d) O and (e) Mn.

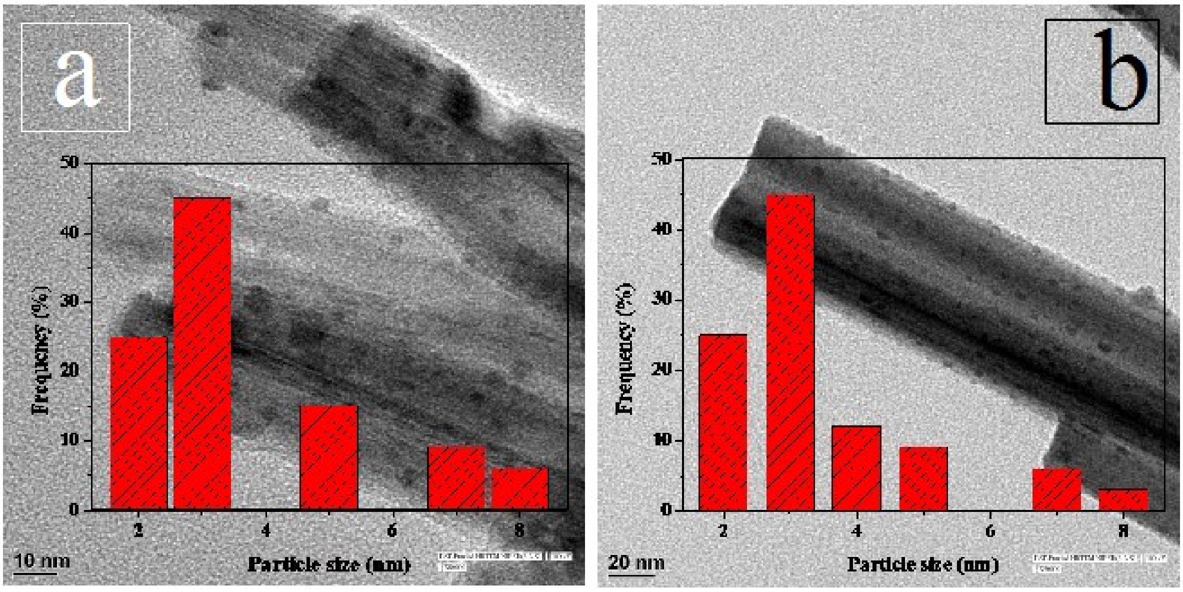

Figure S3. Particle size distributions (histogram) of (a) fresh catalyst (based on Fig. 6b and that of (b) spent catalyst (based on Fig. 6d).

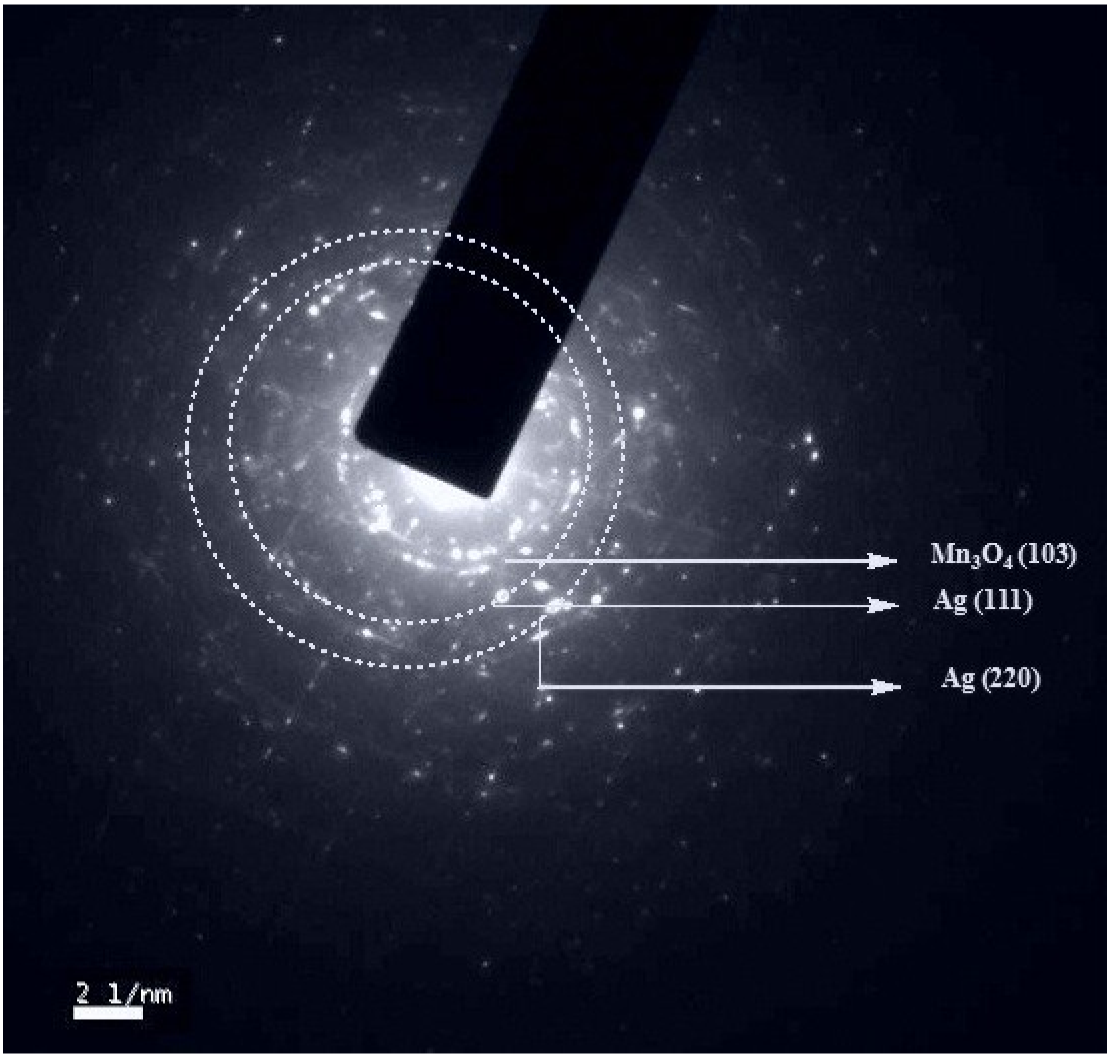

Figure S4. The electron diffraction pattern (based on Fig. 6b, Main).

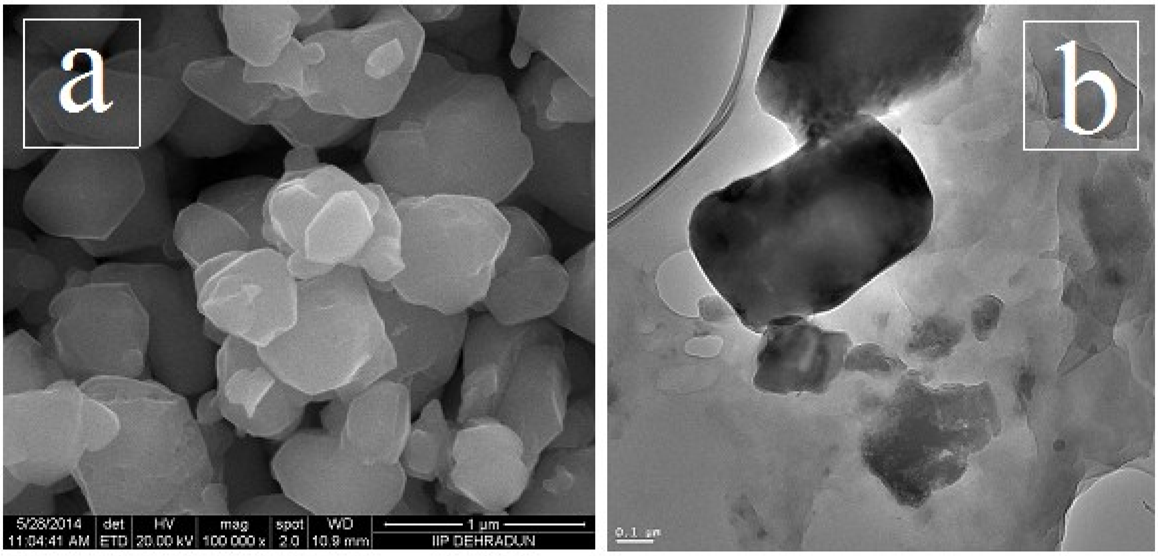

Figure S5. (a) SEM and (b) TEM image of the Ag-Mn catalyst without using the surfactant CTAB.

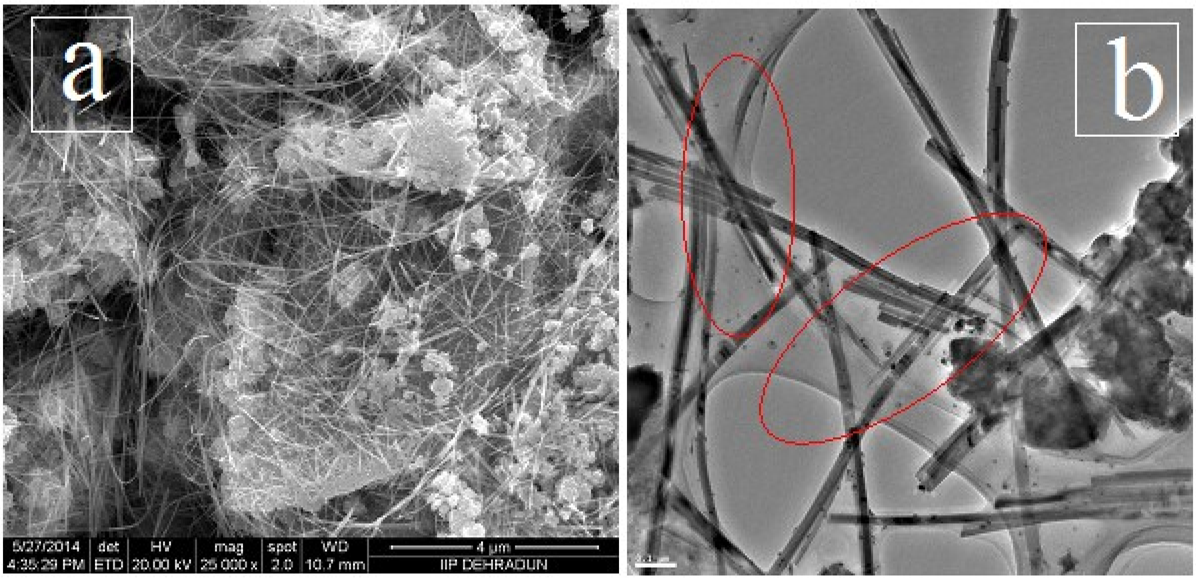

Figure S6. (a) SEM and (b) TEM image of the Ag-Mn catalyst using Ag: CTAB = 1:0.3.

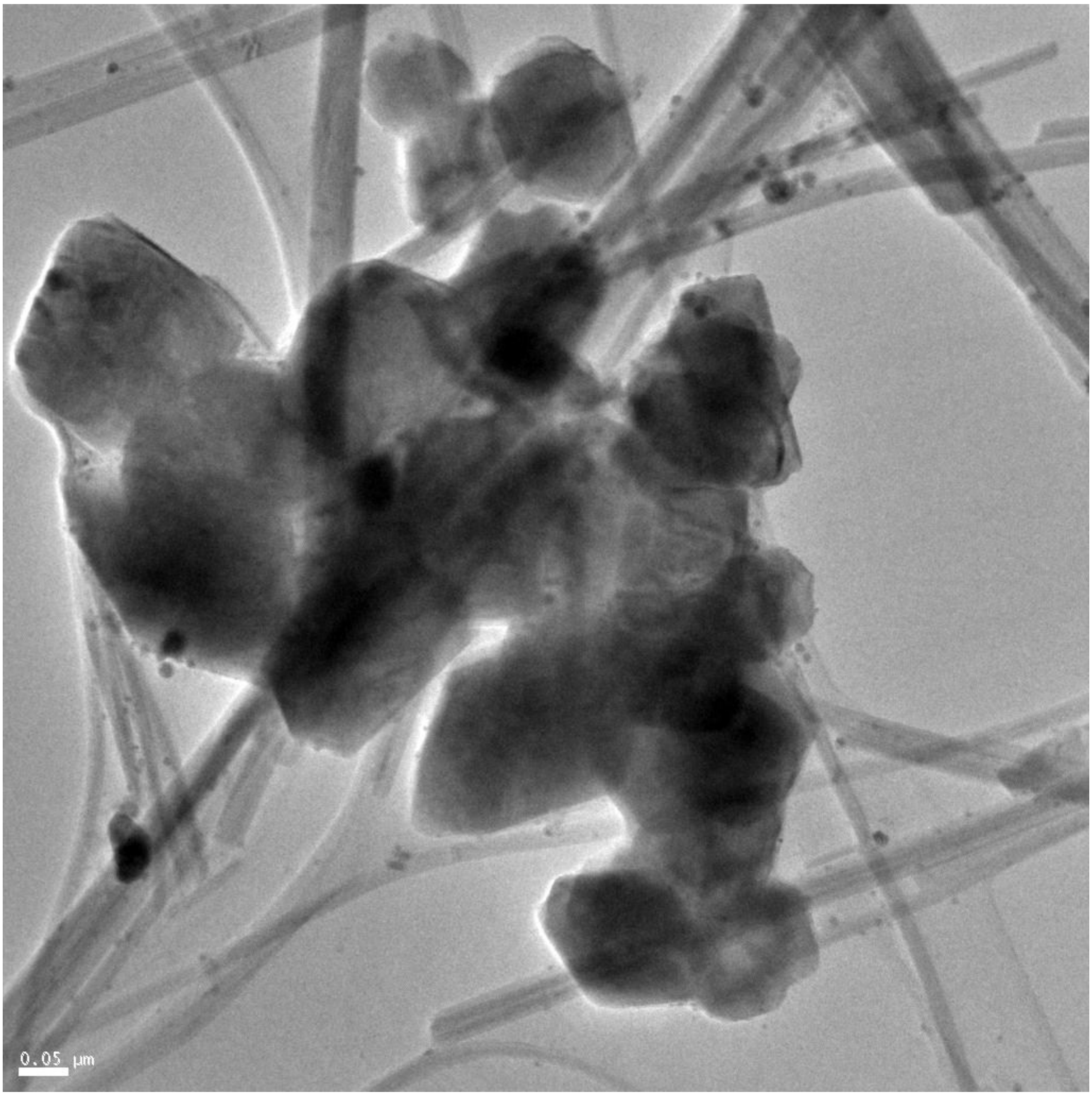

Figure S7. TEM image of the Ag-Mn sample when the aging time was 30 min.

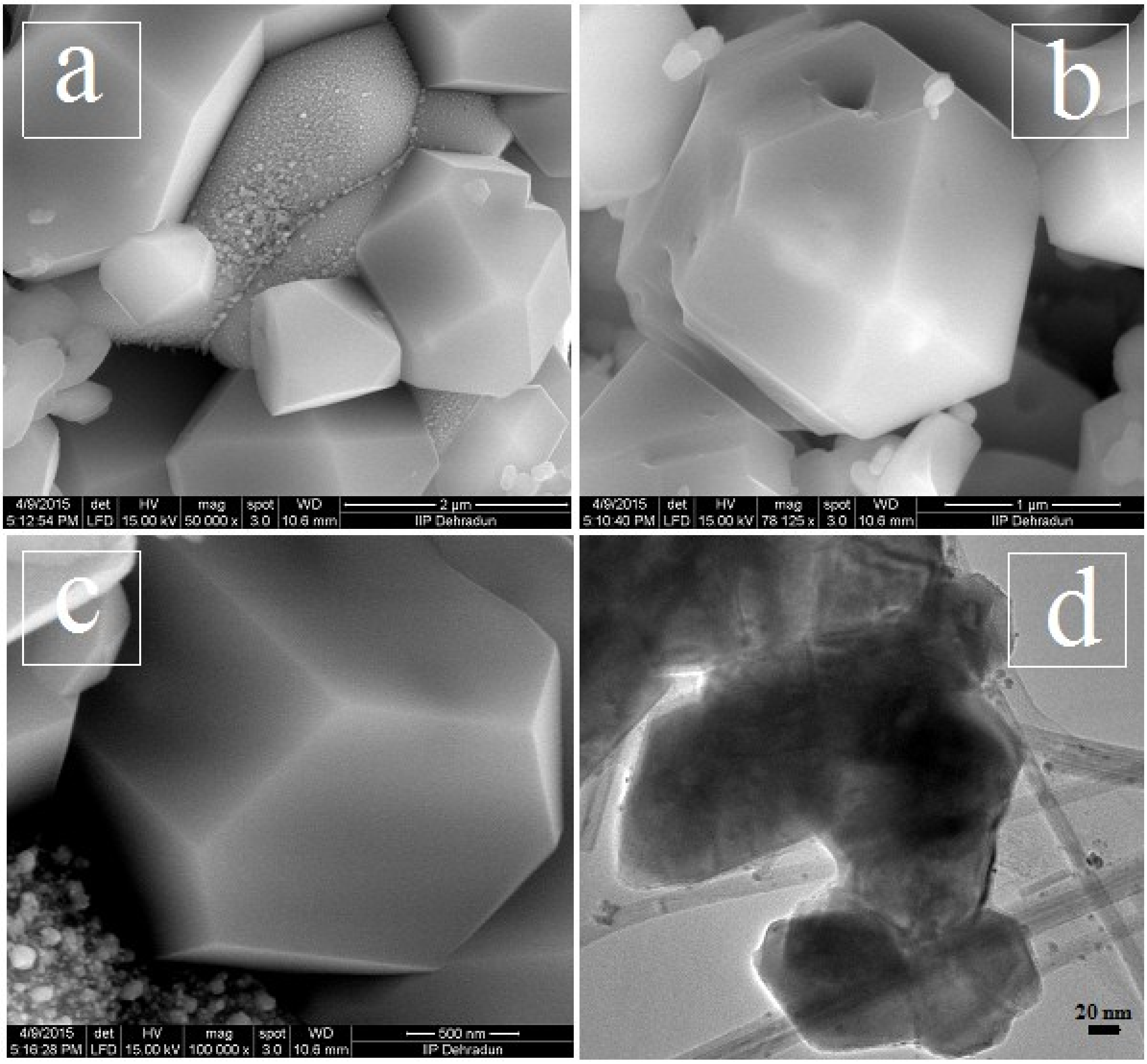

Figure S8. (a-c) SEM and (d) TEM images of the Ag-Mn sample when the aging time prolonged to 24h.

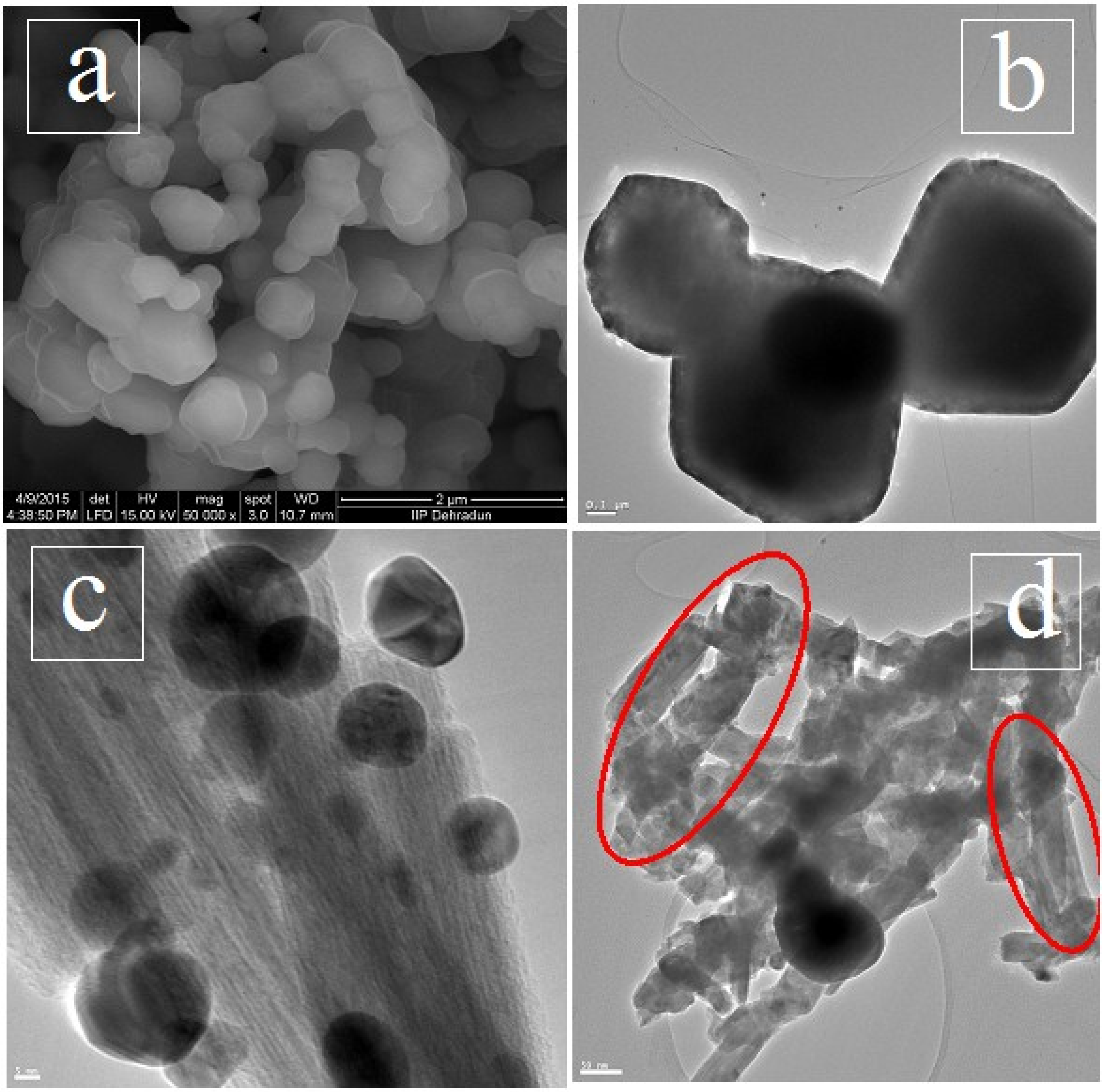

Figure S9. TEM images of the samples with Ag-loadings (a) 0 %, (b) 1.6 % (c) 15.5% and (d) 27%.

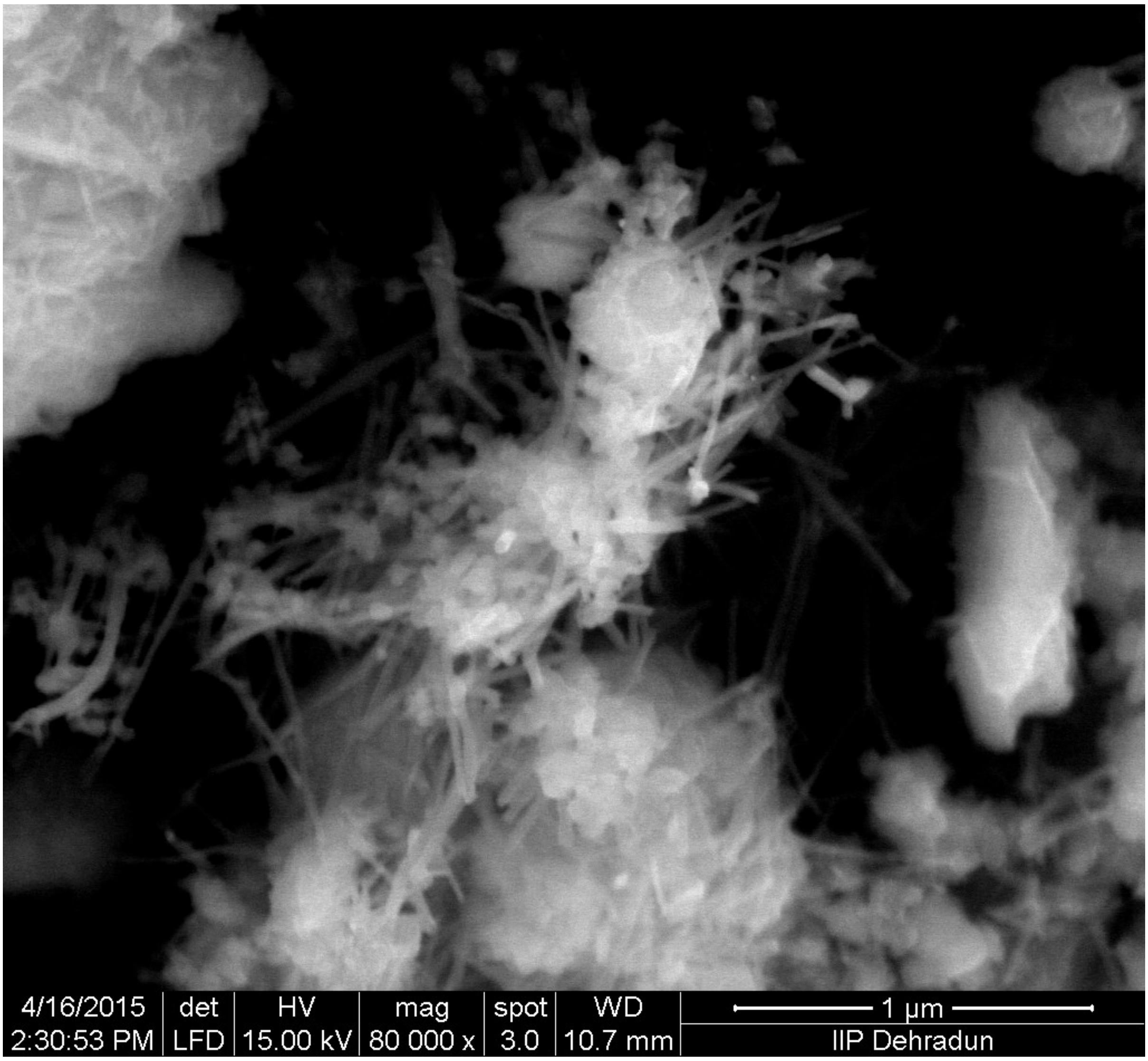

Figure S10. SEM images of the Ag-Mn sample when nitrate precursors of Ag and Mn and cetyl alcohol was used as surfactant.

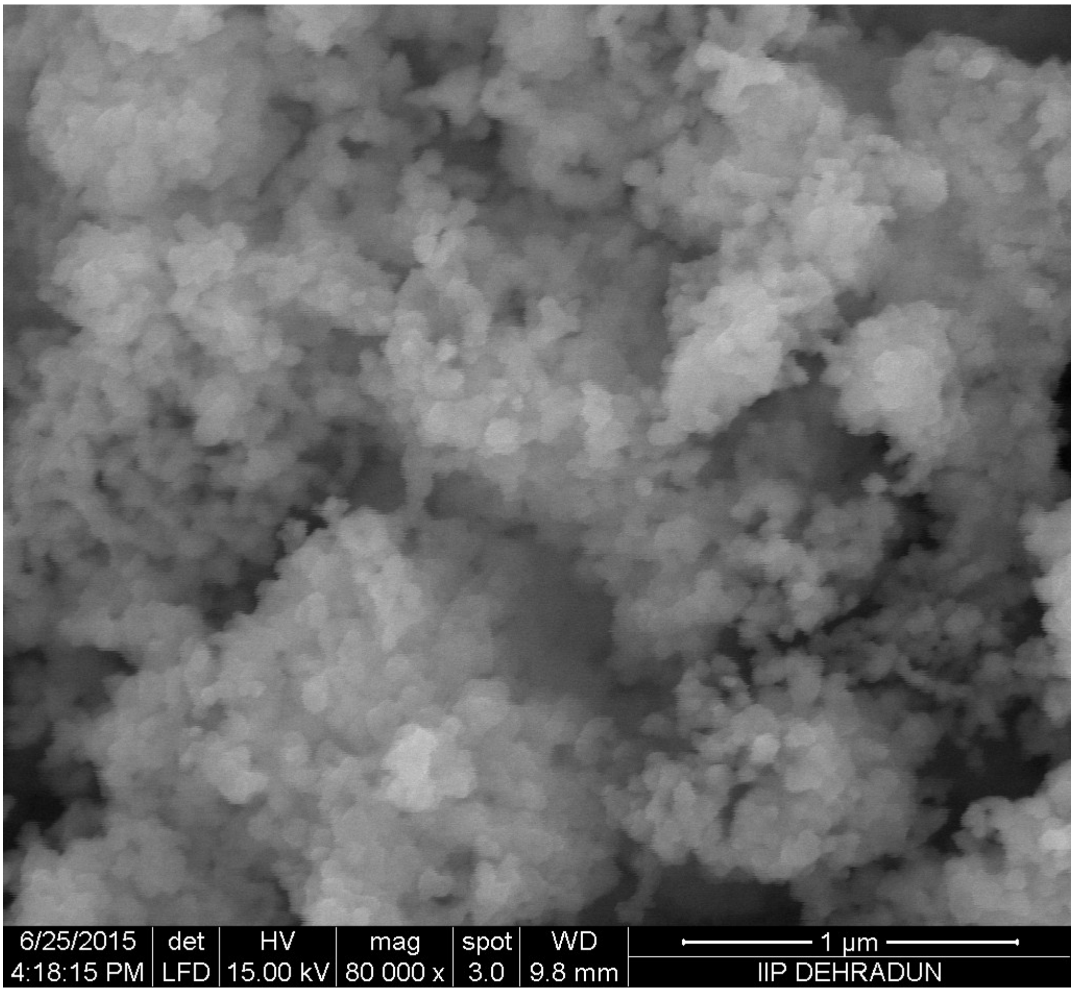

Figure S11. SEM images of the Ag-Mn sample when nitrate precursors of Ag and Mn and sodium dodecylsulfate (SDS) was used as surfactant.

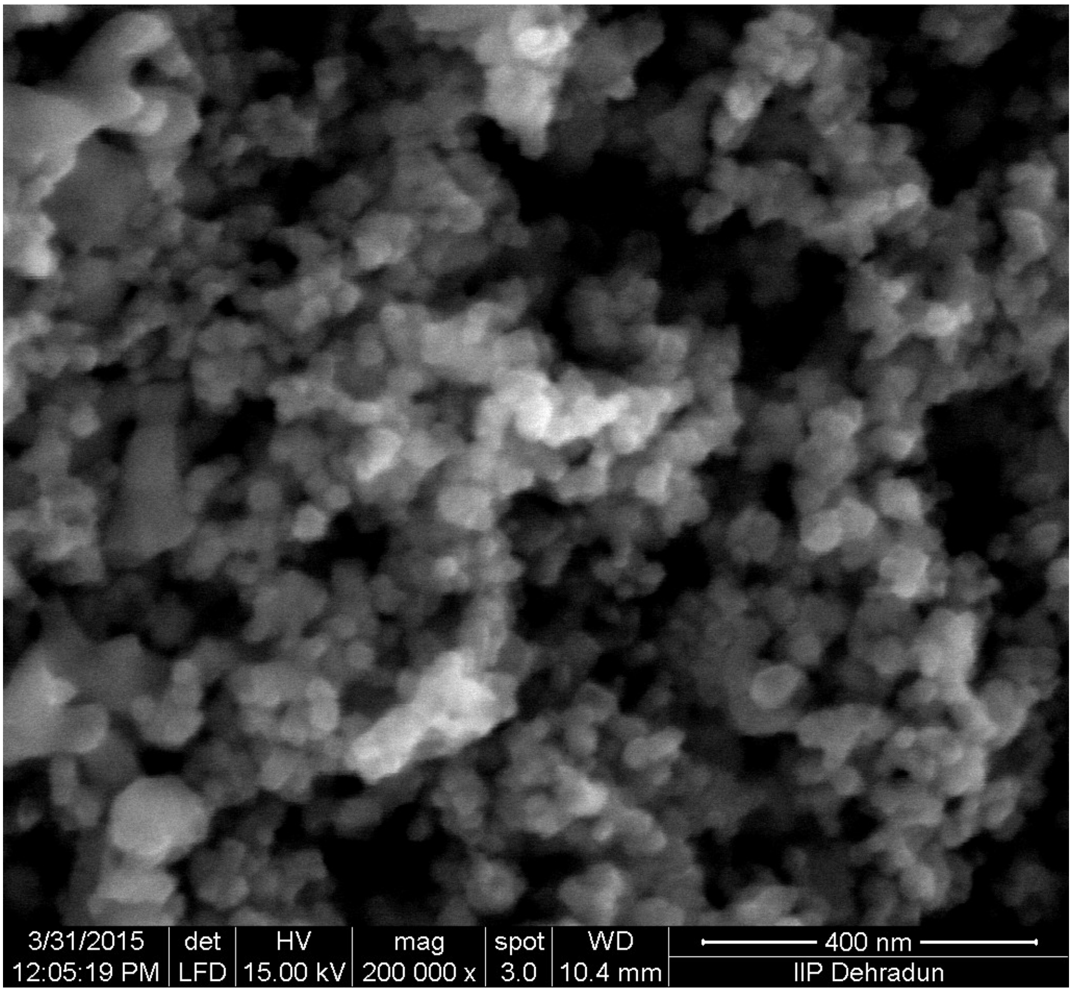

Figure S12. SEM image of the sample taking $KMnO_4$ as the precursor of Mn and avoided the addition of any Ag-species and the other reagents were added as before.

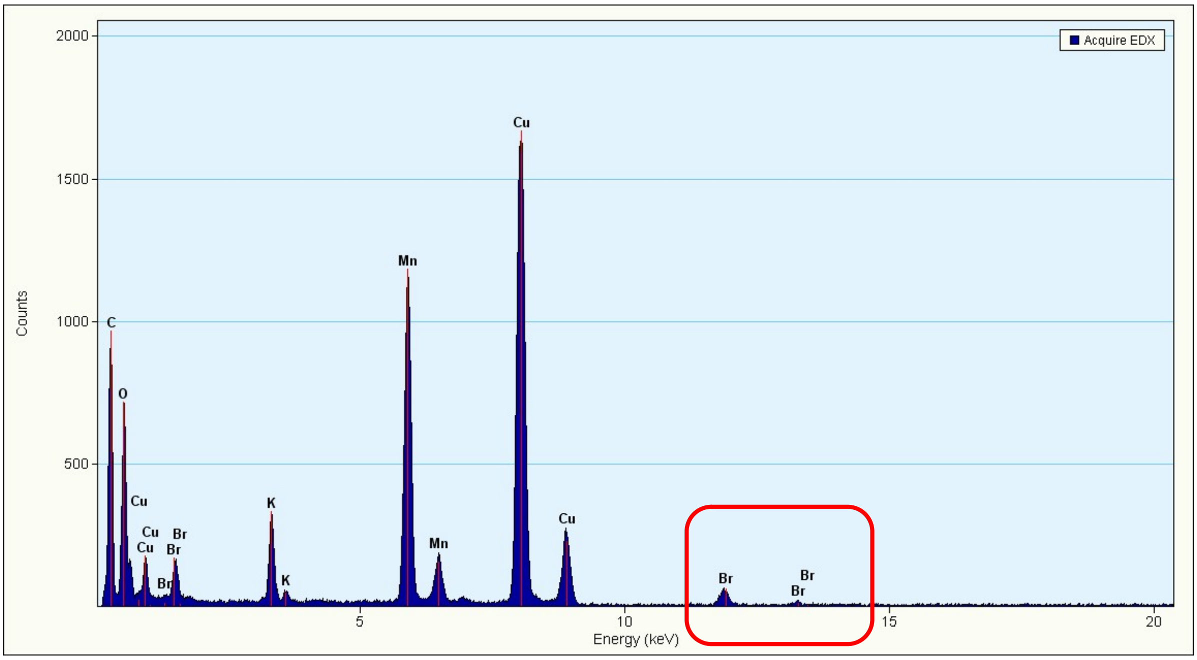

Figure S13. TEM-EDX (based on Figure 10c) of the sample i.e. manganese oxide, which was prepared by the addition of excess KBr solution in $KMnO_4$ + CTAB solution (calined at 500 °C/3h)

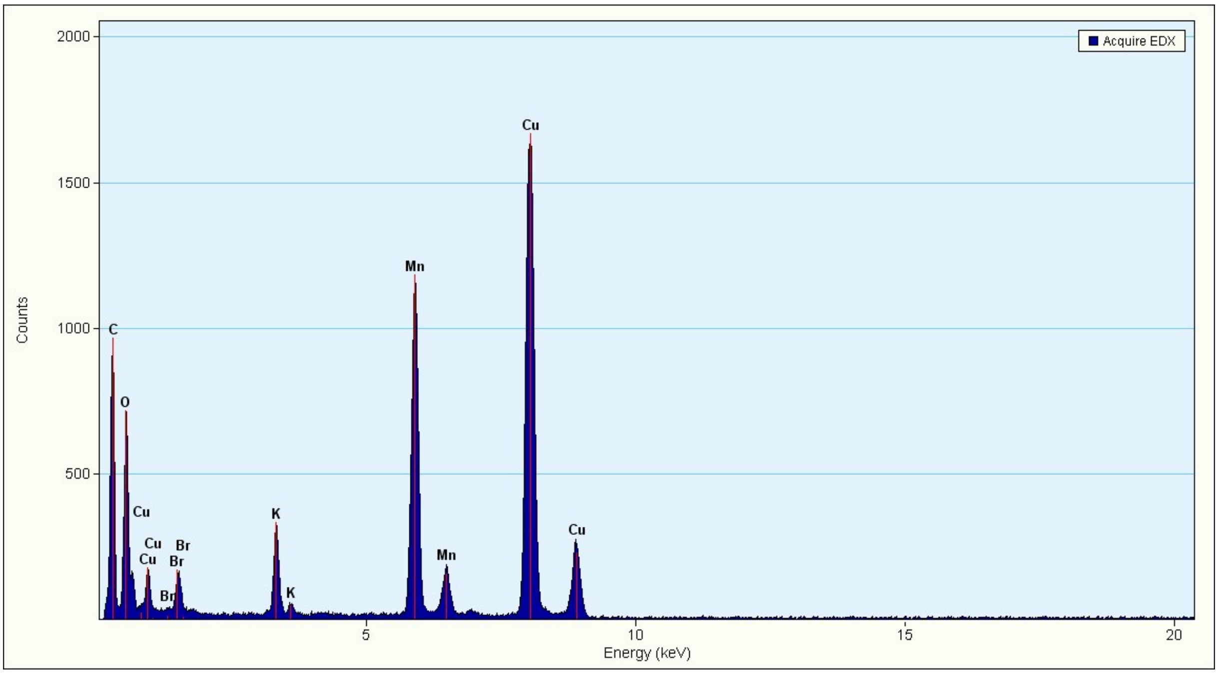

Figure S14. TEM-EDX (based on Figure 10c) of the sample i.e. manganese oxide, which was prepared by the addition of excess KBr solution in $KMnO_4$ + CTAB solution (calined at 500 °C/6h)

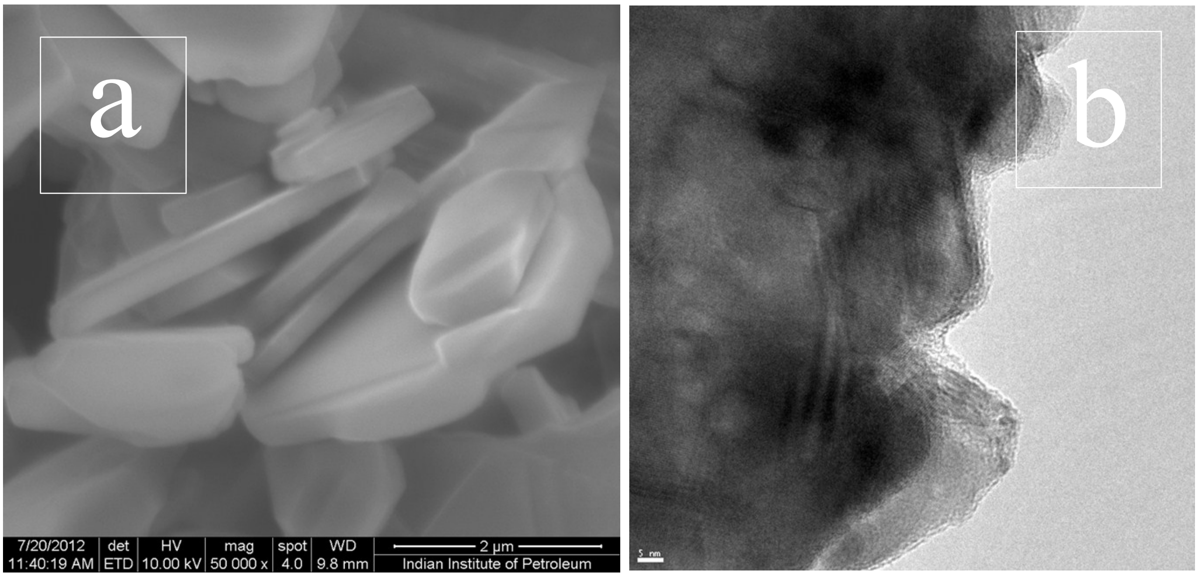

Figure S15. (a) SEM and (b) TEM images of the Ag-Mn sample when $KMnO_4$ was used as the precursor of Mn.

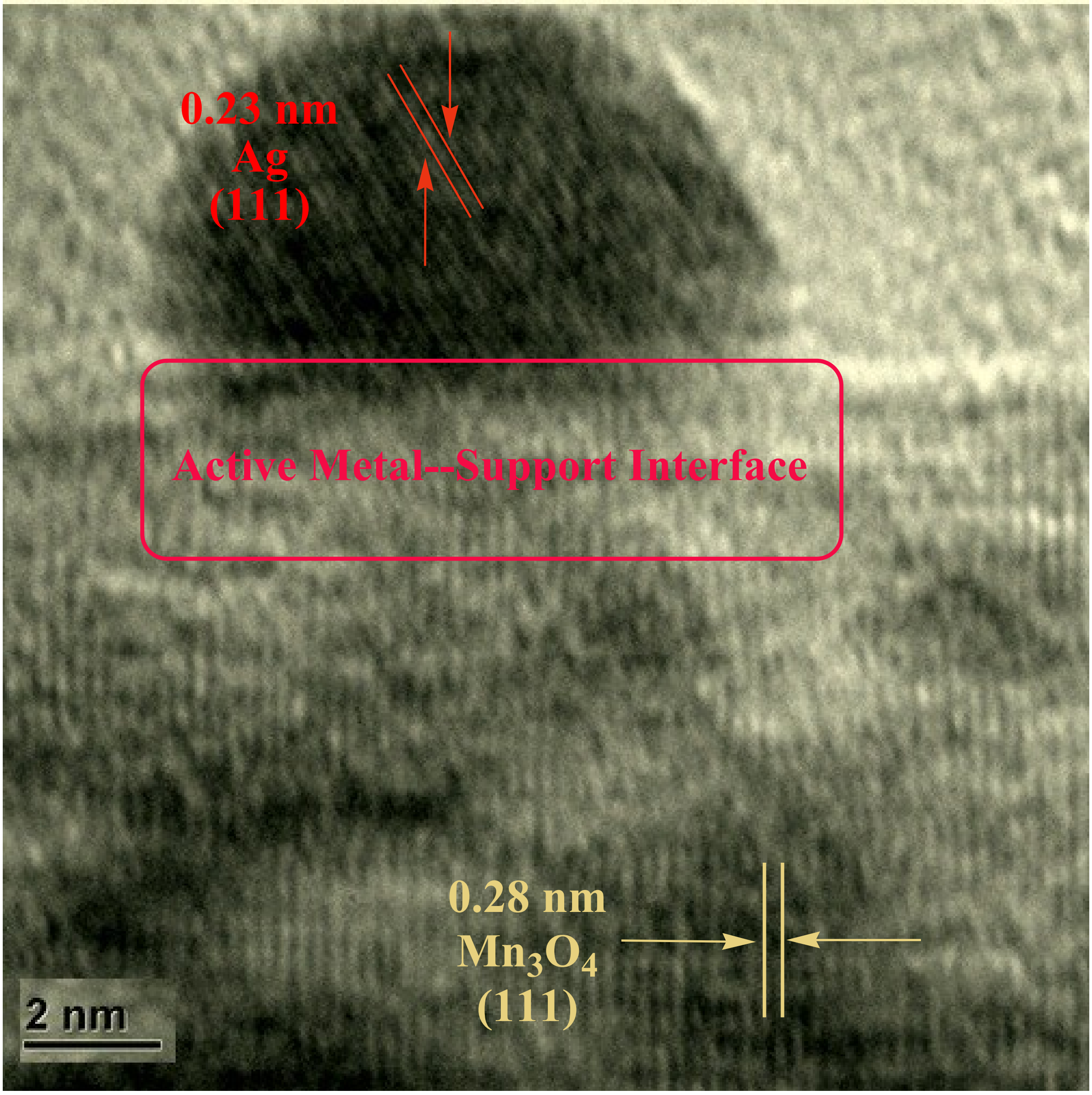

Figure S16. TEM image of the 1D Ag/Mn3O4 catalyst (HRTEM) to show the Ag-Mn interface.